Proceedings of IPACK03
International Electronic Packaging Technical Conference and Exhibition
July 6-11, 2003, Maui, Hawaii, USA

IPACK2003-35151

CONSTRUCTING A TRADE-OFF SURFACE FOR EXTRUDED HEAT SINKS EXPOSED TO FORCED CONVECTION

D.J. de Kock **J.A. Visser**

Department of Mechanical and Aeronautical Engineering
University of Pretoria, Pretoria, 0002, South Africa
Tel: +27 12 420-2448 email: djdekock@postino.up.ac.za

ABSTRACT

In modern electronic components power densities are being increased continuously while the size and weight decrease. The effective dissipating of the heat produced by these components has now become a major design problem. Ordinary heat sinks often used to dissipate this heat, can in many instances no longer be used. Heat sinks therefore need to be designed and optimized for specific applications. The design of these heat sinks requires a difficult trade-off between conflicting parameters, e.g. mass or material cost, maximum temperature and pressure drop. Since these parameters influence one another, optimum designs require the use of mathematical optimization techniques. In the case of heat sinks, the thermal engineer would typically like to optimize the design simultaneously for three design parameters. The parameters are maximum heat sink temperature, mass and pressure drop. In the formulation of such an optimization problem, where more than one design criterion is important, the engineer currently has to assign the relative importance of each design criteria before starting the optimization. A better approach is to perform a range of optimization problems where the relative importance of the design criteria is varied systematically to obtain a trade-off surface of optimum heat sinks. This surface can then be used to investigate the influence of the different design criteria on each other and to select the optimum heat sink for a specific application. In this study such a trade-off surface is created for an extruded heat sink exposed to forced convection. The constructing of this surface is obtained by combining a semi-empirical simulation program, QFin 3.0 with the DYNAMIC-Q optimization method.

INTRODUCTION

The continuing increase of power densities in electronics packages and the simultaneous drive to reduce the size and weight of electronic products have led to an increased importance in thermal management issues in this industry. With the higher outputs, the junction temperature is now often the limiting factor when determining the lifetime of a package. Improved and optimized cooling mechanisms have therefore become a critical part of the electronics industry.

The most common and cost effective method for cooling packages today, is still the use of heat sinks. These heat sinks provide a large surface area for the dissipation of heat and effectively reduce the thermal resistance of a package. Unfortunately, heat sinks often take up much space and contribute significantly to the weight and cost of the product. Heat sinks therefore need to be designed properly and optimized for specific applications.

The thermal performance of a heat sink depends on a number of parameters, including the thermal conduction resistance, dimensions of the cooling channels, location and concentration of heat sources as well as the airflow bypass due to flow resistance through the heat sink. These parameters make the optimal design of a heat sink not a trivial task. Traditionally, the performance of heat sinks is measured experimentally and the results are made available in the form of design graphs in heat sink catalogues. This characterization method has been the topic of much debate as vendors have applied different standards or interpretations to determine the characterization of heat sinks[1,2]. Analytical and empirical formulations for the fin efficiency, pressure drop and the heat transfer coefficient have also been used in the design process to determine the optimal heat sink design. Knight et. al.[3,4] developed and verified a generalized model to determine the optimal geometrical design of closed-fin heat sinks. Lee[5] analytically determined the optimal design of heat sinks by performing a parametric analysis that takes flow bypass into account. Computational Fluid Dynamics (CFD) techniques have been used more frequently in the last few years[6], but

 Copyright © 2003 by ASME

Downloaded From: https://proceedings.asmedigitalcollection.asme.org on 06/28/2019 Terms of Use: http://www.asme.org/about-asme/terms-of-use

mostly on a trial-and-error basis due to the computational cost of performing parametric studies.

A better approach is to combine some sort of a numerical simulation with a mathematical optimization technique, thereby incorporating the influence of the design variables automatically. In a study by Craig et. al.[7] CFD has been used to optimize the mass of a heat sink with a limit on the maximum allowable temperature inside the heat sink. This method has the disadvantage that the computational costs are very high leading to long design cycles. To overcome this problem Visser and de Kock[8] used a semi-empirical thermal simulation program to find the optimum heat sink. In this study the optimum heat sink was defined as the heat sink with either the minimum mass with a limit on the maximum temperature. However, in this study in the definition of the optimum, only one design criteria was optimized while putting a limit on another design criteria.

In this study three design criteria (i.e. maximum heat sink temperature, heat sink mass and pressure drop across the heat sink) are combined during the optimization of the heat sink. Different weights are assigned to the two different design criteria and then optimized. Selecting a range of different weights, constructing the different optimization problems and then optimizing each of the optimization problems separately yields a set of optimum heat sinks or called the Pareto-optimal set. This set can be presented graphically by plotting the different design criteria versus each other. The resulting surface is called a trade-off surface. The thermal engineer can use this trade-off surface to select an optimized heat sink best suited for his application.

PROBLEM DEFINITION AND FORMULATION

The problem considered in this paper is the construction of a trade-off surface (also called the Pareto-optimal set) for an extruded heat sink with a given heat source exposed to forced convection. Once a Pareto-optimal set is generated the thermal design engineer can select from this surface an optimized heat sink that will work best for his application.

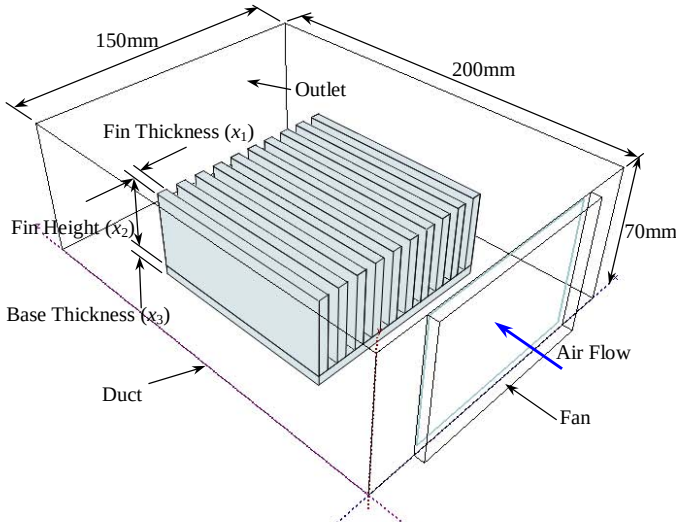

Figure 1: Graphical presentation of design variables

The chosen heat sink with the design variables are depicted graphically in Figure 1. The design variables are fin thickness (x_1), fin height (x_2) and base thickness (x_3). For practical considerations, the design variables are confined to certain prescribed limits. These limits are shown in the results section and are normally derived from manufacturing limitations and geometrical considerations. The limits used here are only illustrative, and in practice would depend on the specific application being considered by the heat sink designer. These constraints, corresponding to the minimum and maximum allowable values for the respective variables, are also referred to as side constraints.

The complete mathematical formulation of the optimization problem using the weighted sum method for multi-objective optimization problems, in which the constraints are written in the standard form $g(\boldsymbol{x}) \le 0$, where $\boldsymbol{x}$ denotes the vector of the design variables $[x_1, x_2, x_3]^T$, is as follows:

$$\text{Minimize } f(\boldsymbol{x}) = \alpha f_1(\boldsymbol{x}) + \beta f_2(\boldsymbol{x}) + \gamma f_3(\boldsymbol{x}) = \alpha \frac{T_{HS}}{T_{HS}^0}(\boldsymbol{x}) + \beta \frac{m_{HS}}{m_{HS}^0}(x) + \gamma \frac{\Delta P_{HS}}{\Delta P_{HS}^0}(\boldsymbol{x})$$

subject to: (1)

$$g_j = -x_j + x_j^{\min} \le 0;\ j = 1,3,5$$

$$g_j = x_j - x_j^{\max} \le 0;\ j = 2,4,6$$

where α, β and γ are weighting factors, T_{HS} is the maximum temperature in the heat sink, m_{HS} is the mass of the heat sink, and ΔP_{HS} is the pressure drop across the heat sink, T_{HS}^0, m_{HS}^0 and ΔP_{HS}^0 are the initial values of the maximum temperature, heat sink mass and pressure drop respectively and lastly $x_j^{\min}$ and $x_j^{\max}$ are the side constraints for the j^{th} variable. The different objectives in Eq. (1) are scaled by their initial values to avoid any difficulties due to the difference in the absolute value of the different objectives.

THEORETICAL MODELING

Thermal Modeling

The thermal modeling is carried out by the semi-empirical thermal simulation program, QFin 3.0[9,10]. The conduction in the heat sink is obtained by numerically solving the curvilinear form of the diffusion equation. In Cartesian co-ordinates the general diffusion equation is:

$$\rho c \frac{\partial T}{\partial t} = \frac{\partial}{\partial x}\left(k \frac{\partial T}{\partial x}\right) + \frac{\partial}{\partial y}\left(k \frac{\partial T}{\partial y}\right) + \frac{\partial}{\partial z}\left(k \frac{\partial T}{\partial z}\right) + S \qquad (2)$$

where ρ is the density of heat sink material, c is the specific heat of the material, k is the thermal conductivity of the material, t is the time when considering transient phenomena, T is the temperature at spatial coordinate (x,y,z) and S is a local source term.

An analytical model proposed by Butterbaugh and Kang[11] was adapted for the purpose of this study to calculate the velocity of the air between the fins and around the heat sink. This is done by considering each flow path in the duct containing the heat sink obstruction, and then determining the

Copyright © 2003 by ASME

Downloaded From: https://proceedings.asmedigitalcollection.asme.org on 06/28/2019 Terms of Use: http://www.asme.org/about-asme/terms-of-use

associated pressure losses in the system (ΔP_{HS}) using a flow network set-up. Thermal boundary conditions are then calculated using compact analytical and empirical models adapted from Van der Pol and Tierney[12]. The heat transfer to the environment accounts for both the convection and radiation. A more detailed description of the fluid and thermal modeling can be found in Ref. [13].

Mathematical Optimization

Pareto-optimal sets are used in this study since the optimization problem considered in this paper is a multi-objective optimization problem. A design vector $\boldsymbol{x}^*$ is part of the Pareto optimum set if and only if, for any $\boldsymbol{x}$ and i:

$$f_j(\boldsymbol{x}) \le f_j(\boldsymbol{x}^*),\ j = 1,\ldots m;\ j \ne i \Rightarrow f_i(\boldsymbol{x}) \ge f_i(\boldsymbol{x}) \qquad (3)$$

In words this means that any point in this set defines a heat sink where any decrease in one of the objectives will result in an increase of one or more of the other objectives.

One of the ways of finding the Pareto-optimal set is through the weighted sum method[14] as given in Eq. (1). This method consists of two parts. The first part is to set-up the different optimization problems that need to be solved to obtain the trade-off surface. This is done by setting up a number of different optimization problems for different choices of the weighting factors (α, β and γ) in the definition of the objective function ($f(\boldsymbol{x})$) as given in Eq. (1).

The second step in finding the Pareto-optimal set is to solve all these constructed optimization problems. The solution of all these optimization problems yields a set of optimum heat sinks called the Pareto-optimal set. These optima can be visualized generating a three dimensional plot of the different components of the objective function ($f_1(\boldsymbol{x})$, $f_2(\boldsymbol{x})$ and $f_3(\boldsymbol{x})$) versus each other. This plot is called the trade-off surface.

As explained above, the second step of the optimization is to solve all these constructed optimization problems to yield the Pareto-optimal set. The optimization method used to solve these problems is the DYNAMIC-Q method[15] as implemented in the optimization module of QFin. This approach involves the application of a dynamic trajectory method for unconstrained optimization[16,17], adapted to handle constrained problems through appropriate penalty function formulations[18]. This DYNAMIC method is applied to successive approximate Quadratic sub-problems of the original problem. The successive sub-problems are constructed from sampling, at relative high computational expense, the behavior of the objective function at successive approximate solution points in the design space. The sub-problems, which are analytically simple, are solved quickly and reliably using the adapted dynamic trajectory method, the latest version of which is described in Ref. [19]. With reference to the current study, the use of approximate sub-problems limits the number of simulations required for the solution of the original optimization problem. A brief outline of the DYNAMIC-Q methodology now follows.

Consider the typical and general inequality constrained optimization problem of the following form:

$$\text{Minimize } f(\boldsymbol{x}), \quad \boldsymbol{x} \in R^n \qquad (4)$$

subject to the following inequality constraints

$$g_j(\boldsymbol{x}) \le 0 \qquad j = 1,2,\ldots,m \qquad (5)$$

and equality constraints

$$h_k(\boldsymbol{x}) = 0 \qquad k = 1,2,\ldots,r \qquad (6)$$

An initial trial design $\boldsymbol{x}^{(0)}$ is available, and t he solution to the problem is denoted by $\boldsymbol{x}^*$.

The penalty function referred to above, is defined by:

$$p(\boldsymbol{x}) = f(\boldsymbol{x}) + \sum_{j=1}^{m} \alpha_j g_j^2(\boldsymbol{x}) + \sum_{k=1}^{r} \beta_k h_k^2(\boldsymbol{x})$$

where

$$\alpha_j = \begin{cases} 0 \text{ if } g_i(\boldsymbol{x}) \le 0 \\ \rho_j = \text{a large positive number for all } j \text{ if } g_j(\boldsymbol{x}) > 0 \end{cases} \qquad (7)$$

and β_k = a large positive number for all k.

For simplicity the penalty parameters, $\rho_j, j = 1,2,\ldots,m$ and $\beta_k, k = 1,2,\ldots,r$, take on the same positive value, $\rho_j = \beta_k = \mu$. It can be shown that, as μ tends to infinity, the unconstrained minimum of $p(\boldsymbol{x})$ tends to the constrained minimum of the original problem defined by Eq. (4)-(6). In the application of the dynamic trajectory method used here [19], and with the objective and gradient functions appropriately scaled, the penalty parameter μ is introduced at a certain specified value, here $\mu = 10^2$, and then increased to $\mu = 10^4$ when the intersection of active constraints is found. Starting with a small value in the penalty parameter ensures that the optimization method is stable while increasing the value, when the intersection of active constraints is found, increases the accuracy of the optimization method. These value of the penalty parameter has been proven to work extremely well[15]. The dynamic trajectory method is applied to approximate sub-problems as follows.

Successive approximate quadratic sub-problems, $P[l] : l = 0,1,2,...$, are formed at successive design points $\boldsymbol{x}^{(l)}$, starting with an initial arbitrary design $\boldsymbol{x}^{(0)}$. For the sub-problem $P[l]$ the approximation $\tilde{f}(\boldsymbol{x})$ to $f(\boldsymbol{x})$ may be given by:

$$\tilde{f}(\boldsymbol{x}) = f(\boldsymbol{x}^{(l)}) + \nabla^T f(\boldsymbol{x}^{(l)})(\boldsymbol{x} - \boldsymbol{x}^{(l)}) + \frac{1}{2}(\boldsymbol{x} - \boldsymbol{x}^{(l)})^T C_j^{(l)} (\boldsymbol{x} - \boldsymbol{x}^{(l)}) \qquad \text{for } j = 1,2,\ldots,m \qquad (8)$$

where $\nabla f(\boldsymbol{x})$ denotes the gradient vector. The approximate Hessian matrix ($\boldsymbol{C}_j^{(l)}$) is given by the diagonal matrix:

$$\boldsymbol{C}_j^{(l)} = diag\left(c_j^{(l)}, c_j^{(l)}, \ldots, c_j^{(l)}\right) = c_j^{(l)} \boldsymbol{I} \qquad (9)$$

This approximation to the Hessian matrix is locally sufficiently accurate.

Copyright © 2003 by ASME

Downloaded From: https://proceedings.asmedigitalcollection.asme.org on 06/28/2019 Terms of Use: http://www.asme.org/about-asme/terms-of-use

The initial values $c_j^{(0)}$ depend on the specific problem being considered. Here a value of 0.0 was arbitrarily used for the first sub-problem implying a linear approximation. Thereafter the $c_j^{(l)}$ are calculated using the expression:

$$c_j^{(l)} = \frac{2\left\{f(\boldsymbol{x}^{(l-1)}) - f(\boldsymbol{x}^{(l)}) - \nabla^T f(\boldsymbol{x}^{(l)})(\boldsymbol{x}^{(l-1)} - \boldsymbol{x}^{(l)})\right\}}{\left\|\boldsymbol{x}^{(l-1)} - \boldsymbol{x}^{(l)}\right\|^2} \qquad (10)$$

where $\|\cdot\|$ denotes the Euclidian norm.

As a further aid in controlling convergence, intermediate move limits are imposed on the design variables during the minimization of the sub-problem. These constraints are described by:

$$\begin{aligned} x_i - x_i^{(l)} - \delta_i \le 0 \\ -x_i + x_i^{(l)} - \delta_i \le 0 \end{aligned} \quad ; \quad i = 1,2,\ldots,n \qquad (11)$$

The approximate sub-problem $P[l]$ constructed at $\boldsymbol{x}^{(l)}$ is then:

$$\begin{aligned} &\text{Minimize } \tilde{f}(\boldsymbol{x}), \quad \boldsymbol{x} \in R^n \\ &\text{subject to} \\ &g_j(\boldsymbol{x}) \le 0 \qquad j = 1,2,...,m \\ &h_k(\boldsymbol{x}) = 0 \qquad k=1,2,...,r \end{aligned} \qquad (12)$$

Additional move limits as given in Eq. (11) and side constraints are also prescribed.

The components of the gradient vector of the objective function in Eq. (1) at a specific design point $\boldsymbol{x}$, with respect to each of the design variables x_i, and used in the construction of the sub-problem are approximated by the first-order forward differencing scheme:

$$\frac{\partial f(\boldsymbol{x})}{\partial x_i} \approx \frac{f(\boldsymbol{x} + \Delta \boldsymbol{x_i}) - f(\boldsymbol{x})}{\Delta x_i} \quad ; \quad i = 1,2,\ldots,n \qquad (13)$$

where $\Delta \boldsymbol{x_i} = [0,0,\ldots,\Delta x_i,\ldots,0]^T$, and Δx_i is a suitable step size determined from a sensitivity study. It is clear that n+1 numerical analyses are required at each design point $\boldsymbol{x}$ to determine all the components of the constraint gradient vectors. The successive simple quadratic sub-problems are solved economically using the latest version of the trajectory method[19] referred to above.

RESULTS AND DISCUSSION

The method outlined above is now applied to a typical extruded heat sink exposed to forced convection. The heat sink consists of a 100×100×5mm base with 10 fins on top of the base. The fins are 5mm thick, 40mm high and 100mm in length. The heat sink is made out of aluminum with a conductivity of 226W/m·K, a density of 2698kg/m^3, a specific heat of 920J/kg·K and an emmisivity of 0.46. The heat source is a 50×50mm square component with a power dissipation of 25W. The heat sink is shown in Figure 1. The heat sink is placed in a 150×200mm rectangular duct with a fan upstream of the heat sink as shown in Figure 1. An ideal fan curve is prescribed and is shown in Figure 2. The air inlet temperature and cabinet temperature was taken as 25°C.

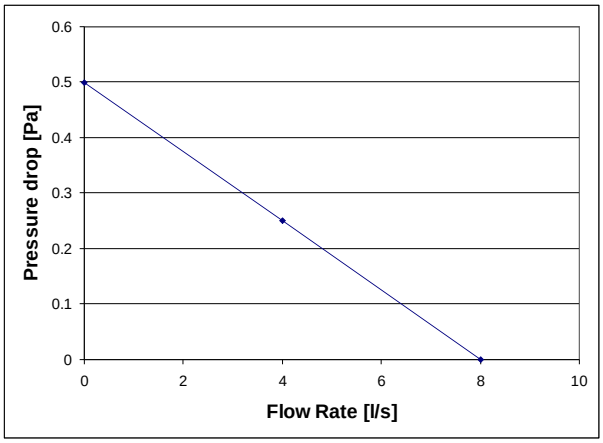

Figure 2: Prescribed ideal fan curve

When solved without any optimization this set-up has a maximum temperature of 58.4ºC, weighs 0.675kg and has a pressure drop of 0.196Pa. The resulting temperature contours for this case is shown in Figure 3 while the pressure on the heat sink surface is shown in Figure 4.

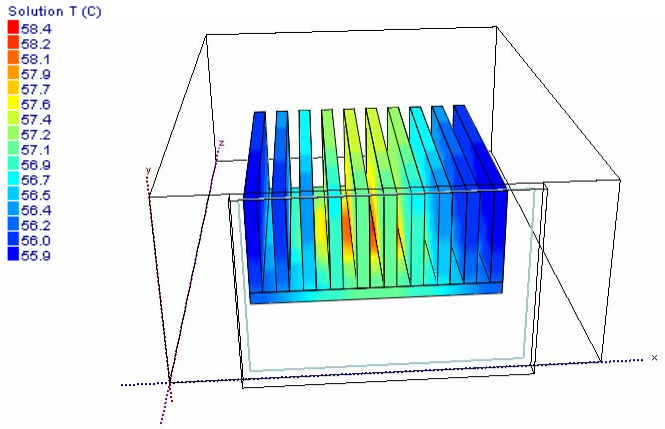

Figure 3: Temperature contours on heat sink for initial set-up

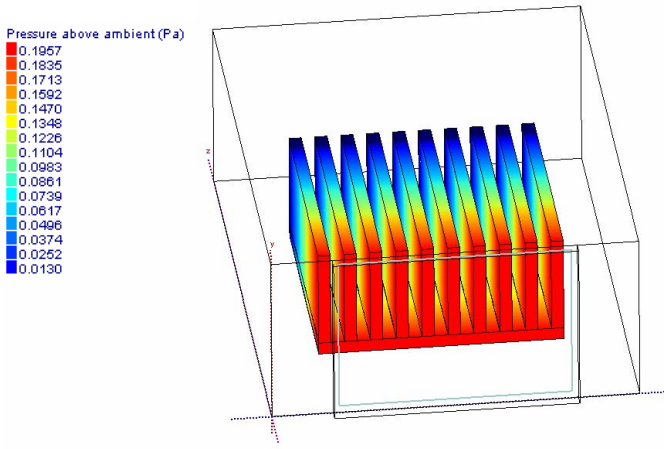

Figure 4: Pressure contours on heat sink for initial set-up

Copyright © 2003 by ASME

Downloaded From: https://proceedings.asmedigitalcollection.asme.org on 06/28/2019 Terms of Use: http://www.asme.org/about-asme/terms-of-use

Three optimization cases studies are considered in this paper. As a step towards constructing the trade-off surface, the first two cases considered are the construction of the trade-off between two objectives only, resulting in a trade-off curve. The last case study, which is the main aim of this study, is the construction of the trade-off between three objectives. The chosen side constraints for all the cases considered are given in Table 1.

Table 1: Side Constraints on the design variables

	Minimum	Maximum
Fin thickness (x_1)	1 mm	7.5 mm
Fin height (x_2)	20 mm	60 mm
Base thickness (x_3)	2 mm	7.5 mm

Case 1: Trade-off curve for maximum temperature vs. heat sink mass

In the first case, the trade-off between the maximum temperature in the heat sink and the heat sink mass is constructed. This is achieved by keeping γ equal to zero and just varying α and β in Eq. (1) when constructing the set of optimization problems to be solved.

The typical convergence history for one of the optimization cases is shown in Figure 5 and Figure 6. The convergence history of the combined objective function as well as the individual objective functions are shown in Figure 5 while the convergence history of the design variables is shown in Figure 6. It can be seen from these figures that the optimization algorithm converges in 5 iterations for this case.

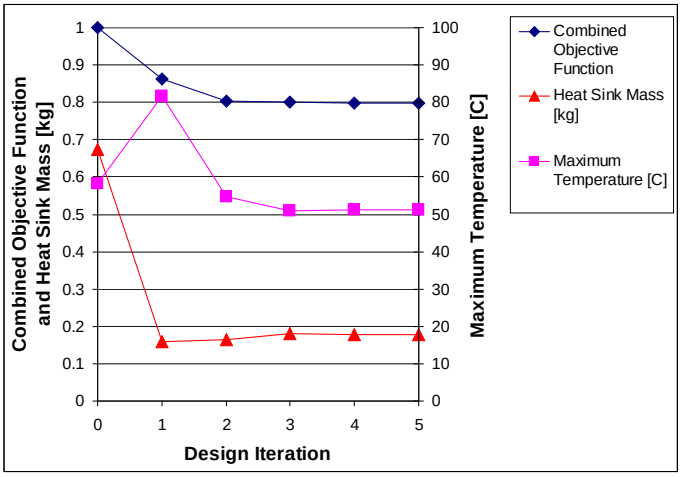

Figure 5: Typical convergence history of objective functions

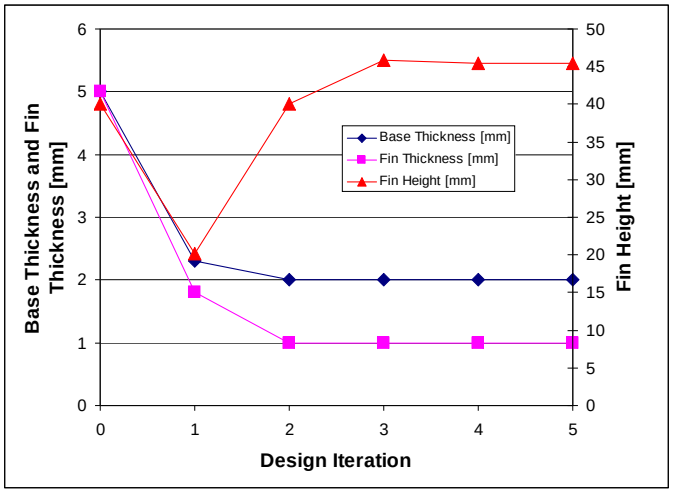

Figure 6: Typical convergence history of design variables

After completing the set of optimization runs for the first case, a trade-off curve was constructed as shown in Figure 7. In this figure the maximum temperature (the 1st objective) is plotted against the heat sink mass (the 2nd objective) to show the trade-off curve. The starting point of the optimization run is shown in this figure by the red square. Also shown in this figure is cross-sectional view of three heat sinks from the Pareto-optimum set.

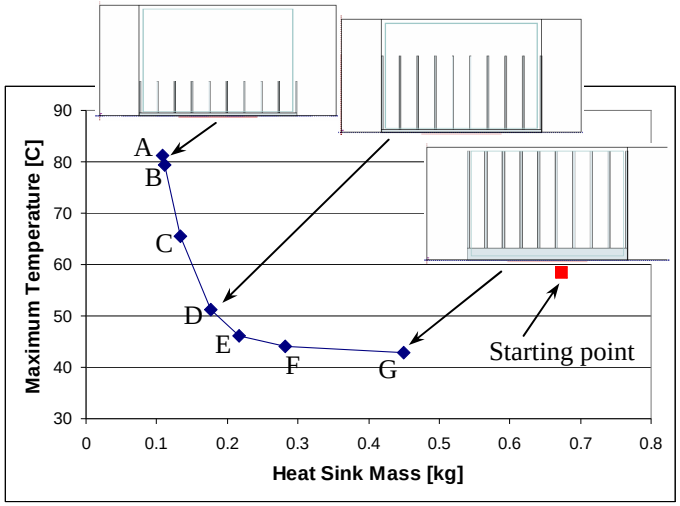

Figure 7: Trade-off curve for maximum temperature vs. heat sink mass

A list of all the optimum heat sinks as represented on the trade-off curve moving from point A to G are given in Table 2. This table gives the value of each of the components of the design vector as well as the maximum heat sink temperature and the heat sink mass.

Copyright © 2003 by ASME

Downloaded From: https://proceedings.asmedigitalcollection.asme.org on 06/28/2019 Terms of Use: http://www.asme.org/about-asme/terms-of-use

Table 2: Different optimum heat sink configurations defining the trade-off curve – Case 1

Point on Curve	α	β	Fin Thickness (x_1) [mm]	Fin Height (x_2) [mm]	Base Thickness (x_3) [mm]	Maximum Temperature (f_1) [°C]	Heat Sink Mass (f_2) [kg]
A	0	1	1.0	20.0	2.00	81.2	0.108
B	0.4	0.6	1.0	20.8	2.00	79.5	0.111
C	0.5	0.5	1.0	28.6	2.00	65.6	0.133
D	0.75	0.25	1.0	45.4	2.00	51.3	0.177
E	0.875	0.125	1.0	59.4	2.00	46.2	0.216
F	0.975	0.025	1.0	60.0	4.40	44.2	0.282
G	1	0	1.5	60.0	7.50	43.0	0.450

One can see that the mass is the dominating objective for point A on the trade-off curve, resulting in a very light heat sink with a high maximum temperature. The dominating objective at point G is the maximum heat sink temperature resulting in a heavier heat sink with a very low maximum temperature. Using the results from Table 2, the thermal engineer can obtain the lightest heat sink configuration that will still meet the thermal requirements of the application. If the maximum allowable temperature in the heat sink is for instance 55°C, option D will be the best available heat sink.

A sensitivity study was done to investigate the effect of the starting point of the optimization on the resulting trade-off curve. For this study the stating point was changed by reducing the base thickness to 4mm, the fin thickness to 2mm and the fin height to 30mm. The resulting trade-off curve together with the first trade-off curve is shown in Figure 8. As can be seen in this figure, the resulting trade-off curve is insensitive for the two different stating points and the two trade-off curves fall on each other.

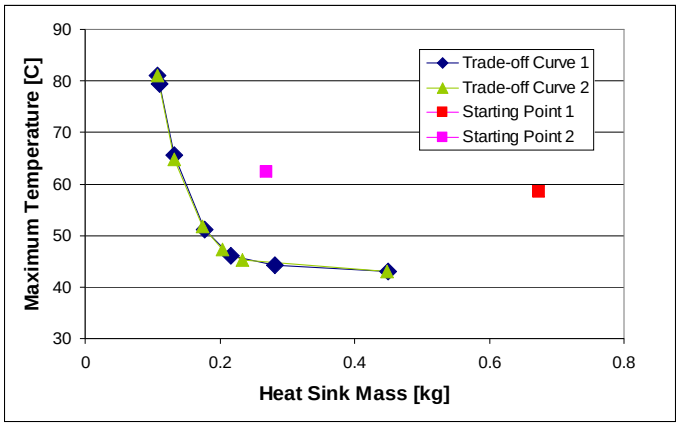

Figure 8: Trade-off curve for maximum temperature vs. heat sink mass for two different starting points

Case 2: Trade-off curve for maximum temperature vs. pressure drop across heat sink

In the second case the trade-off between the maximum temperature and the pressure drop across the heat sink is investigated. This is achieved by keeping β equal to zero and just varying α and γ in Eq. (1) when constructing the set of optimization problems to be solved. The resulting trade-off curve is shown in Figure 9. The starting point of the optimization is again indicated by the red square.

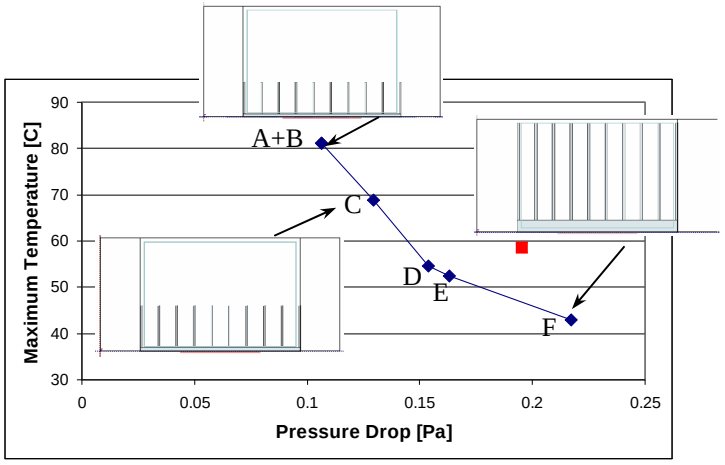

Figure 9: Trade-off curve for maximum temperature vs. pressure drop across heat sink

The list of all the optimum heat sinks as represented on the trade-off curve moving from point A to E are given in Table 3. It can be seen that the trade-off curve for this case tends to be more linear than for Case 1.

Table 3: Different optimum heat sink configurations defining the trade-off curve – Case 2

Point on Curve	α		Fin Thickness (x_1) [mm]	Fin Height (x_2) [mm]	Base Thickness (x_3) [mm]	Maximum Temperature (f_1) [°C]	Pressure Drop (f_3) [Pa]
A	0	1	1.0	20.0	2.0	81.2	0.106
B	0.5	0.5	1.0	20.0	2.0	81.2	0.106
C	0.75	0.25	1.0	26.2	2.2	68.8	0.129
D	0.875	0.125	1.0	38.3	2.9	54.7	0.154
E	0.9	0.1	1.0	41.8	2.9	52.4	0.163
F	1	0	1.5	59.9	7.5	43.0	0.217

Case 3: Trade-off surface for maximum temperature, heat sink mass and pressure drop across heat sink

In the last case study all three objectives were included in the problem formulation. The resulting surface is shown in Figure 10. A surprising result when looking at Figure 10, that instead of having a surface in the three dimensions, all the points fall almost on a three-dimensional curve. This behavior of the graph is caused by the fact that heat sink mass and the pressure drop across the heat sink are not conflicting objectives. In simple words, this means that when the optimization algorithm changes the shape of the heat sink to reduce the mass, the pressure drop decreases at the same time and visa versa. A typical example is that when minimizing the heat sink mass, the fin thickness will be reduced as much as possible. Reducing the fin thickness, also reduces the obstruction in the cabinet and therefore the pressure drop.

Copyright © 2003 by ASME

Downloaded From: https://proceedings.asmedigitalcollection.asme.org on 06/28/2019 Terms of Use: http://www.asme.org/about-asme/terms-of-use

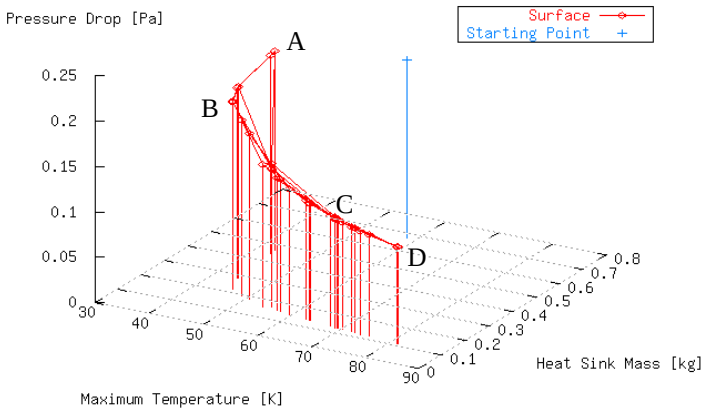

Figure 10: Trade-off surface for maximum temperature, heat sink mass and pressure drop across heat sink

The points on the graph in Figure 10 represent an optimized heat sink where the relative importance of the maximum temperature, heat sink mass and pressure are varied. The thermal design engineer needs to make a selection from one of these optimized heat sinks that will best suite his application.

As an example four of these points are listed in Table 4 and the thermal results in terms of temperature contours in the heat sinks of these points are shown in detail in Figure 11 through Figure 14. The differences in the heat sink profiles can also be seen from these figures.

Table 4: A few samples of the Pareto-optimal set that defines the trade of surface – Case 3

Point on Curve	α	β	γ	Fin Thickness (x_1) [mm]	Fin Height (x_2) [mm]	Base Thickness (x_3) [mm]	Maximum Temperature (f_1) [°C]	Heat Sink Mass (f_2) [kg]	Pressure Drop (f_3) [kg]
A	1	0	0	1.5	60.0	7.5	43.0	0.450	0.217
B	1	0.25	0	1.0	51.1	2.0	48.8	0.195	0.194
C	0.88	0.75	003	1.0	26.9	2.0	68.0	0.128	0.122
D	0	0.75	0.25	1.0	20.0	2.0	81.2	0.108	0.108

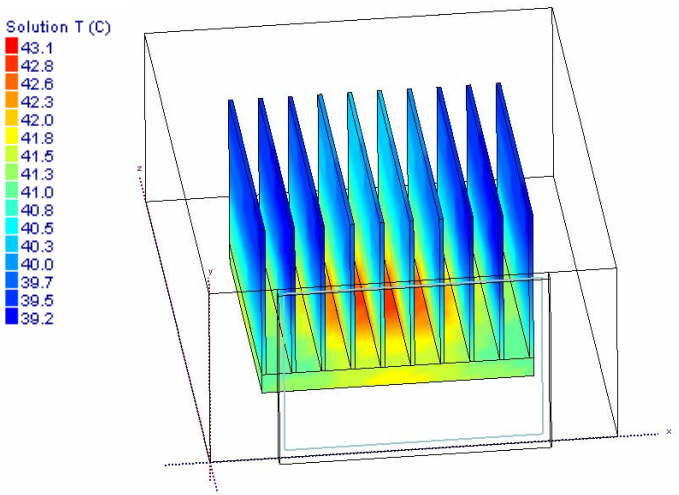

Figure 11: Temperature contours on heat sink for point A

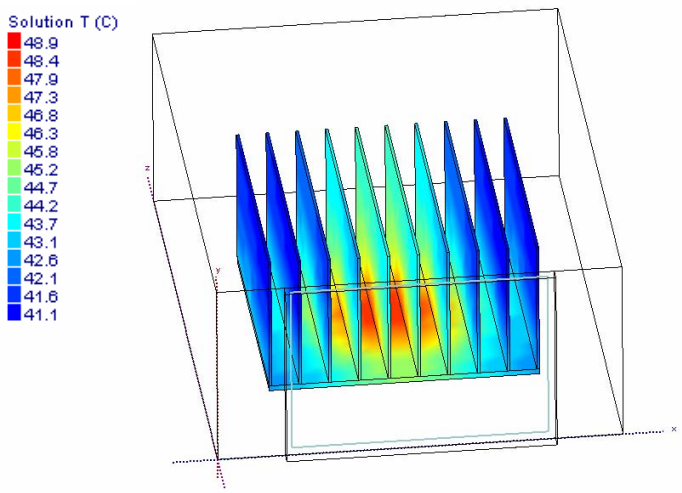

Figure 12: Temperature contours on heat sink for point B

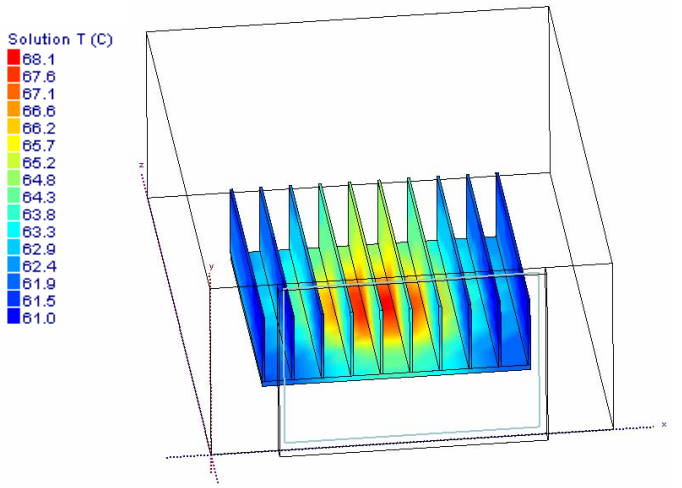

Figure 13: Temperature contours on heat sink for point C

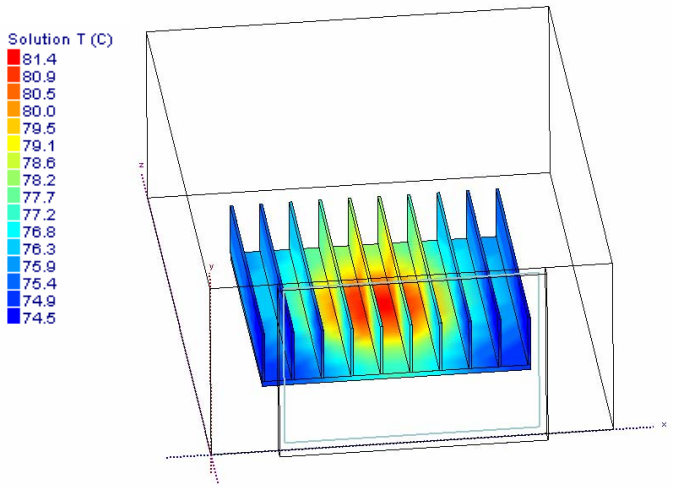

Figure 14: Temperature contours on heat sink for point D

Copyright © 2003 by ASME

Downloaded From: https://proceedings.asmedigitalcollection.asme.org on 06/28/2019 Terms of Use: http://www.asme.org/about-asme/terms-of-use

CONCLUSION AND FUTURE WORK

The paper investigated the construction of a trade-off surface for extruded heat sinks exposed to forced convection. The weighted sum method for construction this surface was used in this study. The DYNAMIC-Q optimization method, combined with the semi-empirical thermal simulation program QFin3.0, proved to be a fast and robust algorithm with convergence reached in fewer than ten design iterations for all the cases considered.

Two trade-off curves were first constructed where the trade-off between the maximum heat sink temperature and heat sink mass; and also the heat sink temperature and pressure drop across the heat sink were investigated. Lastly, the trade-off surface between three objectives was constructed. The three objectives were the maximum heat sink temperature, heat sink mass and pressure drop across the heat sink. The resulting trade-off curves and surface can be used by the thermal design engineer to select an optimized heat sink best suited for his application.

One shortfall of the current implementation in constructing the trade-off surface is the choice of the weighting factors to give an even distribution of points on the trade-off surface. Currently the engineer has to choose the values manually, therefore future work includes the automation of the choices of the different weighting factors to get an even distribution of the Pareto-optimum set. Other heat sink configurations with other design variables, constraints and boundary conditions can also be investigated.

REFERENCES

[1] Kim, S.K., and Lee S., 1997, "On Heat Sink Measurement and Characterisation," *Proceedings of the Pacific Rim/ASME International Intersociety Electronic & Photonic Packaging Conference* (INTERPACK '97), Hawaii.

[2] Biber, C.R. and Belady, C.L, 1997, "Pressure Drop Prediction for Heat Sinks: What is the Best Method?," *Proceedings of the Pacific Rim/ASME International Intersociety Electronic & Photonic Packaging Conference* (INTERPACK '97), Hawaii.

[3] Knight R.W., Goodling, J.S. and Hall, D.J., 1991, "Optimal Thermal Design of Forced Convection Heat Sinks – Analytical," *Journal of Electronic Packaging*, **113**, pp. 313-32.

[4] Knight, R.W., Goodling, J.S. and Gross, B.E., 1992, "Optimal Thermal Design of Air Cooled Forced Convection Finned Heat Sinks - Experimental Verification," *IEEE Transactions on Components, Hybrids, and Manufacturing Technology*, **15**(5), pp. 754-760.

[5] Lee, S., 1995, "Optimum Design and Selection of Heat Sinks," *Proceedings of the 11th Annual IEEE Semi-Therm Symposium*, pp. 48-52.

[6] Obinelo, I.F., 1997, "Characterisation of Thermal and Hydraulic Performance of Longitudinal Fin Heat Sinks for System Level Modeling Using CFD Methods," *Proceedings of the Pacific Rim/ASME International Intersociety Electronic & Photonic Packaging Conference* (INTERPACK '97), Hawaii.

[7] Craig, K.J., de Kock D.J. and Gauché P., 1999, "Minimization of Heat Sink Mass using CFD and Mathematical Optimization," *ASME Journal of Electronic Packaging*, **121**, pp.143-147.

[8] Visser, J.A., and De Kock, D.J., 2002, "Optimization of Heat Sink Mass using the Dynamic-Q Numerical Optimization Method", *Communications in Numerical Methods in Engineering*, **18**, pp. 721-727.

[9] Visser JA, Gauche P., 1996, "A Computer Model to Simulate Heat Transfer in Heat Sinks," *Proc. 4th International Conference for Advanced Computational Methods in Heat Transfer*, Udine, pp. 105-114.

[10] QFin 3.0, 2003, www.qfinsoft.com.

[11] Butterbaugh MA, Kang, SS., 1995, "Effect of Airflow Bypass on the Performance of Heat Sinks in Electronic Cooling," *Advances in Electronic Packaging*, EEP-Vol. 10-2, ASME.

[12] Van de Pol, D.W., and Tierney, J.K., 1974, "Free convection Heat Transfer from Vertical Fin Arrays," *IEEE Transactions on Parts, Hybrids, and Packaging*, **10**(4), pp. 267-271.

[13] Visser, J.A. and De Kock, D.J., 2001, "Optimal Heat Sink Design using Mathematical Optimization," *Proceedings of the Pacific Rim/ASME International Electronic Packaging Technical Conference and Exhibition*, Kauai, Hawaii, USA.

[14] Geoffrion, A.M., 1968, "Proper Efficiency and the Theory of Vector Maximization," *Journal of Mathematical Analysis and Application*, **22**(3), pp. 618-630.

[15] Snyman, J.A., Hay, A.M., 2002, "The DYNAMIC-Q Optimization Method: An Aternative to SQP?" *Computers and Mathematics with Applications*, **44**(12), pp. 1589-1598.

[16] Snyman, J.A., 1982, "A new dynamic method for unconstrained minimization," *Applied Mathematical Modelling*, **6**, pp. 449-462.

[17] Snyman, J.A., 1992, "An improved version of the original leap-frog dynamic method for unconstrained minimization LFOP1(b)," *Appl. Math. Modelling*, **7**, pp. 216-218.

[18] Snyman, J.A., Frangos, C., and Yavin, Y., 1992, "Penalty function solutions to optimal control problems with general constraints via a dynamic optimisation method," *Computational Mathematics and Application*, **23,** pp. 46-47.

[19] Snyman, J.A., 2000, "The LFOPC leap-frog algorithm for constrained optimization," *Computers and Mathematics with Application*; **40**(8/9), pp. 1085-1096.

Copyright © 2003 by ASME

Downloaded From: https://proceedings.asmedigitalcollection.asme.org on 06/28/2019 Terms of Use: http://www.asme.org/about-asme/terms-of-use